NASA TN D-1216

TECHNICAL NOTE

D-1216

STUDY OF A SINUSOIDALLY PERTURBED FLOW IN A LINE INCLUDING A 90° ELBOW WITH FLEXIBLE SUPPORTS

By Robert J. Blade, William Lewis, and Jack H. Goodykoontz

Lewis Research Center
Cleveland, Ohio

NATIONAL AERONAUTICS AND SPACE ADMINISTRATION
WASHINGTON
July 1962

NATIONAL AERONAUTICS AND SPACE ADMINISTRATION

TECHNICAL NOTE D-1216

STUDY OF A SINUSOIDALLY PERTURBED FLOW IN A LINE INCLUDING A 90° ELBOW WITH FLEXIBLE SUPPORTS

By Robert J. Blade, William Lewis,
and Jack H. Goodykoontz

SUMMARY

Sinusoidal acoustic pressure and flow perturbations and related mechanical vibrations were investigated experimentally and analytically in a system consisting of a long hydraulic transmission line with a 90° elbow at the midpoint. The line was supported in a manner that allowed longitudinal movement of the downstream half. A sinusoidal perturbation was imposed on the mean flow at the upstream end by means of small oscillation of a throttle valve about a partially open mean position. The downstream end was terminated in a restricting orifice. Pressure and flow perturbations at both ends of the line and the longitudinal vibration velocity of the downstream pipe section were measured for a range of frequencies.

A method of analysis is presented that is applicable in general to lines consisting of sections of straight pipe connected by bends and supported in a manner permitting longitudinal motion of one or more sections. This method of analysis, which consisted of treating the vibrating pipe section as a viscous-damped spring-mass system and neglecting attenuation of the acoustic waves, was applied to the experimental system with results generally in good agreement with the experimental measurements.

The pipe motion, driven by unbalanced pressure forces on the elbow and the downstream orifice plate, was found to be a major factor in determining the resultant fluid-wave motion. The significant effect of the elbow was solely to provide coupling between the pipe motion and wave motion. Thus, the elbow per se caused no appreciable reflection, attenuation, or phase shift in the fluid waves.

INTRODUCTION

Acoustic pressure and flow perturbations in long hydraulic lines often are of importance in the operation of various fluid systems.

Among these are hydraulic control and rocket propellant systems. If the hydraulic lines are of sufficient length, they will make a significant contribution to the overall dynamic response of the system. Various analyses (refs. 1 and 2) of such systems have been made that show the importance of acoustic effects. Lightweight fluid systems for missile and space applications are more susceptible to acoustic disturbances because of increased mechanical flexibility. Analysis of acoustic effects, therefore, is of increasing importance in the design of these fluid systems.

The results of an experimental study of sinusoidal perturbations of flow in a straight pipe rigidly supported at one end (ref. 3) show that longitudinal wave motion in the material of the pipe wall has a significant effect on the fluid pressure and flow perturbations at frequencies near the quarter-wave resonant frequency of the pipe. A different type of mechanical vibration may occur in hydraulic lines not rigidly supported, containing bends or elbows. A section of the line may vibrate longitudinally as a whole in response to unbalanced mechanical forces resulting from the difference in the fluid pressure perturbations at the two ends of the section.

In this report a method of analysis is proposed to describe acoustic pressure and flow perturbations and associated mechanical oscillations in a fluid transmission line in which a section of pipe is allowed to vibrate longitudinally as a whole. A system in which such vibration could occur was investigated experimentally at the NASA Lewis Research Center, and the results are compared with the analysis of the same system.

The experimental system consisted of a 68-foot-long stainless-steel line (1.00-in. O.D. by 0.065-in. wall) containing a 90° elbow at the midpoint. The line was supported rigidly at the upstream end, and flexible supports were used at the downstream end and at intervals along the line. The experiment covered a range of disturbance frequencies from 0.5 to about 75 cycles per second, mean flow speeds from 5 to 10 feet per second, and mean line pressure from 50 to 225 pounds per square inch. The average amplitude of the sinusoidal perturbation was approximately 5 pounds per square inch for pressure and 0.13 foot per second for fluid velocity. The fluid used was JP-4 fuel. As in the system of reference 3, the flow was modulated by means of a hydraulic servo valve at the upstream end and was restricted by an orifice at the downstream end.

EXPERIMENTAL SYSTEM

Apparatus

Flow system. - The essential parts of the open-loop pumped-return flow system used in the experiment are shown in figure 1. The fluid (JP-4) was forced through the test line by a gear pump, and the mean

flow rate was measured by means of a rotameter. Hydraulic accumulators were placed between the pump and the test line to provide steady supply pressure. The discharge from the test line was submerged in a constant-height vented tank. Fluid was returned to the supply tank by intermittent operation of the return pump.

Flow disturbance generator. - Sinusoidal perturbations of flow and pressure were induced in the system by means of an electrohydraulic servo-actuated throttle valve located just upstream of the test line. The throttle was oscillated sinusoidally about a partially open mean position in response to an alternating voltage. A porous-metal filter was placed between the throttle and the test line to reduce turbulence.

Test line. - The test line, made of stainless-steel tubing, 1.00 inch in outside diameter with a 0.065-inch wall thickness, was 68 feet long and had a sharp 90° elbow at the midpoint. A schematic diagram of the test line is shown in figure 2. The upstream end was attached to the throttle valve, which in turn was rigidly fastened to the ground. The downstream end was attached to the outlet tank by means of a neoprene diaphram, which allowed axial motion but suppressed transverse motion. Between the ends, the test line rested on horizontal transverse wires spaced at 1-foot intervals. The test line was terminated in an orifice plate containing 34 holes 0.040 inch in diameter. The instrument sensing elements and the orifice plate were attached rigidly to the end of the tube. Thus, the test-line suspension allowed longitudinal oscillation of the downstream half of the line (section CE, fig. 2) including the instruments and orifice plate.

Instrumentation. - Instrument sensing elements to measure pressure and flow perturbations were located at stations A and E (fig. 2). The pressure sensors were commercial flush-diaphragm units. Pressure perturbations in pounds per square foot were obtained by means of static calibrations of each unit with its associated amplifier. The flow-perturbation sensors were hot-wire anemometers specifically designed for use in liquid (ref. 3). It was not practicable to obtain static calibrations of the hot-wire sensors because the response is linear only for small perturbations and the sensitivity is a function of the mean fluid velocity. For this reason separate normalizing factors were determined for each run to make the measured impedance equal the calculated value for frequencies from 2 to 4 cycles per second.

The displacement of position of the downstream half of the line was measured with a linear variable differential transformer located at station D. The displacement amplitude in feet was obtained by means of a static calibration of the differential transformer and its associated amplifier. The vibration velocity V in feet per second was calculated from the sinusoidal displacement for each frequency. Provision was also made for the measurement of mean gage pressure at both ends of the line.

The output of the pressure, fluid-flow, and pipe-displacement sensors was in the form of alternating-current electrical signals with phase and amplitude determined by the perturbation of the quantity being measured. These alternating-current signals were amplified and supplied to a commercial transfer-function analyzer which indicated and partially analyzed the data. This instrument effectively rejects all frequencies (noise, distortion, etc.) except the reference frequency and indicates the reference-frequency signal in resolved-component form.

The transfer-function analyzer consisted of two units: (1) an oscillator, which supplied (a) the signal for the servo-throttle flow-disturbance generator and (b) a four-phase reference voltage to the resolved component indicator, and (2) a resolved-component indicator, which indicated the in-phase and quadrature (90° out of phase) components of the pressure, flow, and displacement signals with respect to the reference voltage.

Procedure

The flow system was operated at constant mean flow rate and pressure until conditions had stabilized. Mean gage pressure readings were taken at stations A and E, and the mean flow rate was read on the rotameter. The servo throttle was operated at a series of frequencies from 0.5 to about 75 cycles per second. The amplitude of the throttle area variation was maintained constant over the entire range of frequencies for each run and was kept small relative to the mean open area to avoid nonlinear effects. At each frequency the values of the in-phase and quadrature components of the five dynamic parameters (upstream and downstream pressure and flow, and pipe position perturbations: P_A, P_E, Q_A, Q_E, and X_p) were read in succession on the resolved-component indicator. The mean pressure drop across the downstream orifice was constant during each run, but was changed from run to run to vary the orifice impedance.

The following dimensionless transfer functions were computed from the data to show the relations among the measured quantities. (All symbols are defined in appendix A.)

(1) The dimensionless upstream acoustic impedance:

$$z_A = \frac{P_A}{Z_0 Q_A} \tag{1}$$

(2) The interterminal pressure ratio:

$$\Phi = \frac{P_A}{P_E} \tag{2}$$

(3) The dimensionless downstream mechanical admittance:

$$\Upsilon = \frac{Z_0 SV}{P_E} = \frac{\rho c V}{P_E} \tag{3}$$

In the foregoing equations Z_0 is the characteristic acoustic impedance of fluid waves in the pipe given by

$$Z_0 = \frac{\rho c}{S} \tag{4}$$

The value of the sonic speed c used to determine Z_0 was 3750 feet per second. This value was determined by correcting the value used in reference 3 (3850 ft/sec) for the difference in mean temperature between the two series of experiments (approx. 16° F). The rate of change of sonic speed with temperature (-6 ft/(sec)(°F)) was obtained from data on the density and bulk modulus of hydrocarbons given in reference 4. The density of the fluid was 1.5 slugs per cubic foot, and the internal area of cross section of the line was 0.00413 square foot; hence, Z_0 was calculated to be 1.36×10^6 pound-second per (foot)^5.

ANALYSIS

Method of Analysis

The proposed method of analysis is applicable in general to hydraulic transmission lines composed of sections of straight pipe connected by bends or elbows in such a manner that some longitudinal motion of one or more sections is permitted. It is assumed that one end of the line is terminated in a known impedance; that is, the relation between pressure and flow perturbations at one end of the line is assumed known. If a sinusoidal perturbation of flow or pressure, or both, is impressed at the other end of the line, the resulting perturbations of flow and pressure at all points in the line and the perturbation of position of the movable pipe section(s) will be periodic at the same frequency and approximately sinusoidal. The dynamic behavior of the system is to be described by means of transfer functions giving the relations among the various perturbations in terms of phase and amplitude as a function of the impressed frequency. Methods of calculating these transfer functions are described in the following analyses.

Assumptions. - Analysis of the system is facilitated by making the following simplifying assumptions:

(1) Undamped sinusoidal acoustic waves exist in the fluid.

(2) Longitudinal expansion or compression does not occur in the pipe walls.

(3) The longitudinal motion of a section of pipe vibrating as a whole can be described by the equations for a perfect viscous-damped spring-mass system.

(4) The mean fluid flow speed is negligible compared with the sonic speed.

(5) The terminating impedance at one end of the line is known as a function of frequency.

The applicability of the method is limited to systems in which the assumptions are approximately fulfilled. For example, the assumption of undamped waves may exclude systems employing highly viscous fluids or very small diameter lines. The assumption of no longitudinal compression and expansion is equivalent to neglecting sonic waves in the pipe wall. (The sonic velocity in steel is about four times that in JP-4). The applicability of the results is therefore limited to frequencies well below the lowest natural resonant frequency of longitudinal wave motion in the walls of any straight-pipe section not rigidly supported at both ends.

Outline of method of analysis. - Essential steps in the analysis procedure are the following:

(1) The mechanical forces on the moving pipe section(s) are expressed in terms of the pressure perturbations at the two ends and are related to the pipe velocity perturbation by means of the mechanical impedance of the moving pipe, regarded as a viscous-damped spring-mass system.

(2) The acoustic equations for undamped sound waves are used to relate the pressure and flow perturbations at the two ends of each straight-pipe section (fixed or moving). The flow perturbations are defined with respect to a fixed coordinate system, and the mean fluid flow speed is neglected.

(3) Equations based on continuity of pressure and flow including the flow equivalent of the pipe motion are used to relate conditions in adjoining pipe sections.

(4) The relation between flow and pressure at one end of the line is defined by an expression for the impedance in terms of frequency.

(5) The equations obtained in the preceding steps are solved to obtain expressions for the desired transfer functions.

Analysis of Experimental System

Pressure and flow variations introduced by the oscillating throttle valve and reflected at the exit orifice set up a wave pattern in the line in which the pressure perturbation at the elbow is generally different from the exit pressure perturbation. This pressure difference causes the section of pipe from C to D (fig. 2) to vibrate longitudinally, and the vibratory motion modifies the flow perturbations.

The description of fluid waves in the line by means of the usual equations of acoustics requires that the flow perturbations be referred to a fixed system of coordinates. Accordingly, fixed reference stations B, C, and D (fig. 2) have been selected. Stations B, C, and D are introduced for use in the analysis, whereas stations A and E represent the locations of the instruments attached to the pipe. Station A, like B, C, and D, is fixed with respect to the ground as the pipe is rigidly supported at that point; but station E, the exit measuring station, is not fixed but moves with the pipe. Measured values of flow at station E, therefore, represent flow with respect to the moving pipe.

Steps (1) to (5) of the analysis procedure outlined previously were applied to the system shown in figure 2 as follows:

Step (1): Relation of pressure perturbations to pipe motion. - The pressure perturbations at the ends of pipe section CE provide a net longitudinal driving force in the direction C → E given by

$$F = S[P_E(1 - \epsilon) - P_C] \tag{5}$$

where $S(1 - \epsilon)$ is the area of the solid portion of the orifice plate (excluding the holes). Being flexibly supported, section CE responds with a longitudinal vibration velocity V. The transfer function relating F to V is the mechanical impedance Z_m:

$$Z_m = \frac{F}{V} = \frac{S[P_E(1 - \epsilon) - P_C]}{V} \tag{6}$$

For an ideal viscous-damped spring-mass system the mechanical impedance is given by

$$Z_m = D + i\left(2\pi fM - \frac{K}{2\pi f}\right) \tag{7}$$

where D is the resistance coefficient, M the mass, and K the stiffness.

Step (2): Pressure-flow relations in straight-pipe sections. - In the section of pipe from A to B the pipe vibration is at right angles to

the flow and therefore is assumed to have a negligible effect on the longitudinal wave motion. In the section from C to D the pipe motion is parallel to the flow and, except for frictional effects which are neglected in the analysis, has no influence on the wave motion in a fixed coordinate system. In the pipe sections AB and CD, therefore, the equations for undamped sound waves in uniform pipes are applicable, and the following sets of relations (derived in appendix B using assumptions (1) and (4)) are obtained.

Equations relating conditions at opposite ends of section AB:

$$\left.\begin{aligned} P_B &= P_A \cosh i\beta - Z_0 Q_A \sinh i\beta \\ Z_0 Q_B &= Z_0 Q_A \cosh i\beta - P_A \sinh i\beta \\ P_A &= P_B \cosh i\beta + Z_0 Q_B \sinh i\beta \\ Z_0 Q_A &= Z_0 Q_B \cosh i\beta + P_B \sinh i\beta \end{aligned}\right\} \tag{8}$$

Equations relating conditions at opposite ends of CD:

$$\left.\begin{aligned} P_D &= P_C \cosh i\beta - Z_0 Q_C \sinh i\beta \\ Z_0 Q_D &= Z_0 Q_C \cosh i\beta - P_C \sinh i\beta \\ P_C &= P_D \cosh i\beta + Z_0 Q_D \sinh i\beta \\ Z_0 Q_C &= Z_0 Q_D \cosh i\beta + P_D \sinh i\beta \end{aligned}\right\} \tag{9}$$

The dimensionless frequency parameter β appearing in equations (8) and (9) is defined by

$$\beta = \frac{2\pi f \frac{l}{2}}{c} \tag{10}$$

This parameter represents the phase shift (in radians) occurring in the distance $l/2$ for a single sinusoidal wave train of frequency f and propagation speed c. Introducing the wavelength λ in equation (10) gives

$$\beta = \frac{\pi l}{\lambda} \tag{11}$$

showing that β is proportional to the ratio of line length to wavelength.

Step (3): Continuity relations for pressure and flow. - The velocity of the fluid at station C is the sum of the velocity of the fluid with respect to the pipe and the velocity of the pipe. The velocity of the fluid with respect to the pipe is the same at C as at B; therefore, the flow-continuity relation at the elbow is

$$\frac{Q_C}{S} = \frac{Q_B}{S} + V \tag{12}$$

The assumption that there is no damping at the elbow is expressed by

$$P_C = P_B \tag{13}$$

Similar equations describe the conditions of continuity between stations D and E as follows:

$$P_D = P_E \tag{14}$$

$$\frac{Q_E}{S} = \frac{Q_D}{S} - V \tag{15}$$

Step (4): Impedance at station E. - The imaginary component of the orifice-plate impedance, caused by inertial reaction to changes in flow, has been calculated to be between 10^{-4} and 10^{-5} times the characteristic impedance. To a very close approximation, therefore, the exit-orifice impedance Z_E is real and equal to the slope of the steady-state pressure-flow curve at the operating pressure. Thus, the relation between pressure and flow perturbations at the exit station is

$$\frac{P_E}{Q_E} = Z_E \tag{16}$$

Step (5): Determination of transfer functions. - It is desirable to describe the characteristics of a transmission line in terms of relations among the variables that are observable at the terminals of the line. These variables are P_A, Q_A, P_E, Q_E, and V. The relations among these variables are described by dimensionless transfer functions including the dimensionless upstream impedance $z_A = P_A/Z_0Q_A$, the interterminal pressure ratio $\Phi = P_A/P_E$, and the dimensionless downstream mechanical admittance $T = V\rho c/P_E$. Expressions for these functions were found from equations (6) to (16) by means of algebraic and trigonometric manipulation shown in appendix B. The subscripts x and y are used to denote the real and imaginary components of a complex number; for example, $\Phi = \Phi_x + i\Phi_y$. The results are given in terms of the dimensionless

frequency parameter β (eq. (10)), the dimensionless mechanical impedance z_m is defined by

$$z_m = \frac{Z_m}{\rho c S} \tag{17}$$

and the dimensionless exit impedance z_E is defined by

$$z_E = \frac{Z_E}{Z_0} = \frac{Z_E S}{\rho c} \tag{18}$$

Equations for calculating the four transfer functions are

$$\left.\begin{aligned} \left(\frac{V\rho c}{P_E}\right)_x &= \Upsilon_x = \frac{z_{m,x}(1 - \epsilon - \cos\beta) - (z_{m,y} + \sin\beta)\dfrac{\sin\beta}{z_E}}{z_{m,x}^2 + (z_{m,y} + \sin\beta)^2} \\ \left(\frac{V\rho c}{P_E}\right)_y &= \Upsilon_y = \frac{-(z_{m,y} + \sin\beta)(1 - \epsilon - \cos\beta) - \dfrac{z_{m,x}\sin\beta}{z_E}}{z_{m,x}^2 + (z_{m,y} + \sin\beta)^2} \end{aligned}\right\} \tag{19}$$

$$\left.\begin{aligned} \left(\frac{P_A}{P_E}\right)_x &= \Phi_x = \cos 2\beta - \Upsilon_y(\sin 2\beta - \sin\beta) \\ \left(\frac{P_A}{P_E}\right)_y &= \Phi_y = \frac{\sin 2\beta}{z_E} + \Upsilon_x(\sin 2\beta - \sin\beta) \end{aligned}\right\} \tag{20}$$

$$\left.\begin{aligned} \Psi_x &= \frac{\cos 2\beta}{z_E} + \Upsilon_x(\cos 2\beta - \cos\beta) \\ \Psi_y &= \sin 2\beta + \Upsilon_y(\cos 2\beta - \cos\beta) \end{aligned}\right\} \tag{21}$$

$$\left.\begin{aligned} \left(\frac{P_A}{Z_0 Q_A}\right)_x &= z_{A,x} = \frac{\Phi_x\Psi_x + \Phi_y\Psi_y}{\Psi_x^2 + \Psi_y^2} \\ \left(\frac{P_A}{Z_0 Q_A}\right)_y &= z_{A,y} = \frac{\Phi_y\Psi_x - \Phi_x\Psi_y}{\Psi_x^2 + \Psi_y^2} \end{aligned}\right\} \tag{22}$$

Equations (19) to (22) together with the definitions of β, z_m, and z_E (eqs. (10), (17), and (18)) show that the performance of the system can be calculated if the parameters ρ, c, S, and l are given and Z_m and Z_E are known as functions of frequency. The physical and geometrical constants ρ, c, S, and l can be presumed to be known, and the downstream impedance Z_E can be found from the orifice curve.

The mechanical impedance Z_m of the moving pipe section was found from equation (7) using for M the actual mass of pipe section CE including the fittings and instrument sensors at station E. The stiffness of the suspension κ was obtained from static measurements of force and displacement, and the resistance coefficient D was calculated from the dynamic test data using values of P_E and V for a narrow range of frequencies about the natural resonant frequency. Thus, the pipe motion was represented by a viscous-damped spring-mass system with the following parameters:

Mass, M, slug	0.82
Stiffness, κ, lb/ft	5450
Resistance coefficient, D, lb-sec/ft	21
Undamped natural frequency, cps	13
Dimensionless damping factor, ζ	0.16

RESULTS AND DISCUSSION

The analytical results are presented in figure 3 in the form of phase and amplitude of the several transfer functions plotted against the dimensionless frequency parameter β for values of the dimensionless downstream impedance from 0.6 to 1.3. The functions presented in figure 3 are the dimensionless downstream pipe-motion admittance $V\rho c/P_E$ calculated from equation (19), the interterminal pressure ratio P_A/P_E from equation (20), and the dimensionless upstream impedance P_A/Z_0Q_A from equation (22). The mechanical resonant frequency of the pipe section was 13 cycles per second, and the corresponding value of β is $0.236\ \pi$.

Experimental values of phase and amplitude of $V\rho c/P_E$, P_A/Z_0Q_A, and P_A/P_E are shown in figures 4, 5, and 6 plotted as a function of the frequency parameter β. The plotted points in figures 4 to 6 were determined from the experimental data, and the solid curves are the analytical results obtained by interpolation from figure 3. The dotted curves show for comparison the calculated response for a stationary straight line of the same total length. The agreement between the results of experiment and analysis is considered excellent. The experimental data points follow the pattern of response given by the moving-pipe analysis, and both show substantial departures from the calculated response of a stationary line.

Effect of the Elbow

The generally good agreement between the experimental and analytical results shown in figures 4 to 6 clearly demonstrates that the effect of the elbow on the dynamics of the fluid system arises primarily from the interaction between mechanical and acoustic disturbances. The elbow provides a coupling mechanism whereby fluid pressure perturbations give rise to longitudinal forces on the piping, and pipe motion modifies the fluid flow perturbation. The analysis was based on the assumption that this was the only effect, that is, that the elbow, if stationary, would not cause any reflection, attenuation, or phase shift in the fluid waves. The agreement is sufficiently good to warrant the conclusion that the effect of the elbow per se was negligible compared with the effect of pipe motion.

Mechanical Response of Pipe

The fact that the pipe velocity was substantially as calculated for an ideal viscous-damped spring-mass system is shown by the results in figure 4. The admittance function $V\rho c/P_E$ is referred to the downstream pressure perturbation P_E instead of the effective driving pressure $[P_E(1 - \epsilon) - Pc]$. Thus, the curves of figure 4 represent the response of a second-order system to a variable driving force.

Effect of Pipe Motion on Fluid Waves

The general nature and extent of the effect of pipe motion on the upstream impedance and the interterminal pressure ratio can be shown by a comparison with the calculated response of a rigid system. The latter case, shown by the dotted lines in figures 5 and 6, was determined by setting the pipe velocity equal to zero, making $\Upsilon = 0$ in equations (20) and (21). This procedure gives the familiar equations for undamped fluid waves in a stationary straight line. A comparison of the dotted and solid curves in figures 5 and 6 shows that pipe motion has a significant effect on both the upstream impedance and the interterminal pressure ratio throughout the range of frequency included in the experiment. Typical maximum differences between the moving and stationary systems are 25 percent and 25° (0.14 π). The details of the curves are not of general interest because they apply only to the specific system used in the experiment. However, these results demonstrate that longitudinal pipe motion produces significant changes in the fluid-wave pattern, and that grave errors may be incurred if the effect of pipe motion is neglected. The method of analysis used herein provides a correct description of the response of the system.

CONCLUDING REMARKS

The results of this investigation show that, in a fluid transmission line in which longitudinal motion of a section of piping is allowed, pressure forces will make this section of pipe move, and the resulting motion will have a significant effect on the dynamic response of the line.

The method of analysis proposed herein allows the calculation of this effect by treating the moving pipe as a lumped-parameter vibrating system interacting with undamped acoustic waves in the fluid. Application of the method is limited to frequencies at which distributed-parameter vibrations in the material of the pipe walls can be neglected. The elbow per se caused no noticable reflection, attenuation, or phase shift in the fluid waves.

Lewis Research Center
National Aeronautics and Space Administration
Cleveland, Ohio, Feburary 15, 1962

E-1281

APPENDIX A

SYMBOLS

(Note: Quantities that are in general complex are so noted.)

c	sonic speed, ft/sec
D	effective viscous-damping resistance coefficient, lb-sec/ft
F	vibrotive force, lb (complex)
f	frequency, cps
l	total length of line, ft
M	mass of vibrating portion of pipe, slugs
P	pressure perturbation, lb/sq ft (complex)
Q	volume-flow perturbation, cu ft/sec (complex)
S	area of cross section, sq ft
V	vibration velocity, ft/sec (complex)
X_p	perturbation of pipe position, ft (complex)
Z	acoustic impedance, $Z = P/Q$, lb-sec/ft^5 (complex)
Z_0	characteristic acoustic impedance, $Z_0 = \rho c/S$, lb-sec/ft^5
Z_m	mechanical impedance, $Z_m = F/V$, lb-sec/ft (complex)
z	dimensionless acoustic impedance, $z = Z/Z_0$, (complex)
z_m	dimensionless mechanical impedance, $z_m = Z_m/\rho cS$, (complex)
β	dimensionless frequency parameter, $\beta = \pi f l/c$, radians
ϵ	ratio of area of holes in orifice plate to interior cross section of pipe

ζ	dimensionless damping factor, $\zeta = D/2\sqrt{MK}$
K	stiffness of pipe suspension, lb/ft
λ	wavelength, ft
ρ	density, slugs/cu ft
Υ	dimensionless downstream mechanical admittance defined by $\Upsilon = \rho cV/P_E$ (complex)
Φ	interterminal pressure ratio defined by $\Phi = P_A/P_E$ (complex)
Ψ	dimensionless interterminal admittance defined by $\Psi = Z_O Q_A/P_E$ (complex)

Subscripts:

A, B, C, D, E	stations shown in fig. 2
x	real part of complex number
y	imaginary part of complex number
+	wave moving downstream
-	wave moving upstream

APPENDIX B

DERIVATIONS

Derivation of Acoustic Equations Relating Pressure and Flow Perturbations at Two Points in a Tube

It is shown in textbooks in acoustics (ref. 5) that the relation between the pressure and flow perturbations in an undamped sinusoidal wave train moving in the positive direction in a tube of infinite length and uniform area is

$$\frac{P_+}{Q_+} = Z_0 \tag{B1}$$

For a similar wave train moving in the negative direction,

$$\frac{P_-}{Q_-} = - Z_0 \tag{B2}$$

If a sinusoidal perturbation of flow or pressure is introduced anywhere in the system, the pressure and flow perturbations at any station may be represented by the sum of two sinusoidal wave trains moving in opposite directions, the relative amplitude and phases of the two components being determined by the boundary conditions. Equations relating the pressure and flow perturbations at stations A and B, separated by a uniform section of tube of length $l/2$, are developed as follows.

Adding the effects of the positive- and negative-moving waves gives the resultant pressure and flow perturbations at station A:

$$P_A = P_{+A} + P_{-A} \tag{B3}$$

$$Q_A = Q_{+A} + Q_{-A} \tag{B4}$$

Using equations (B1) and (B2) with (B4) gives

$$Z_0 Q_A = P_{+A} - P_{-A} \tag{B5}$$

and from (B5) and (B3),

$$P_{+A} = \frac{1}{2} (P_A + Z_0 Q_A) \tag{B6}$$

$$P_{-A} = \frac{1}{2}(P_A - Z_0 Q_A) \tag{B7}$$

By using the convention that the direction from A to B is positive and the assumptions that the waves are undamped and the mean flow speed is negligible compared with the sonic speed, there is obtained for the positive-moving wave at station B:

$$P_{+B} = P_{+A}e^{-i\beta} \tag{B8}$$

where β is the lag in phase at B compared with A. In the case of the negative-moving wave the phase at B leads A by the same angle; therefore,

$$P_{-B} = P_{-A}e^{+i\beta} \tag{B9}$$

The total-pressure perturbation at B is

$$P_B = P_{+B} + P_{-B} = P_{+A}e^{-i\beta} + P_{-A}e^{+i\beta}$$

Using equations (B6) and (B7),

$$P_B = \frac{1}{2}(P_A + Z_0 Q_A)e^{-i\beta} + \frac{1}{2}(P_A - Z_0 Q_A)e^{+i\beta}$$

$$P_B = P_A \cosh i\beta - Z_0 Q_A \sinh i\beta \tag{B10}$$

The flow perturbation at B is found in a similar way:

$$Q_{+B} = Q_{+A}e^{-i\beta}$$

$$Q_{-B} = Q_{-A}e^{+i\beta}$$

Multiplying by Z_0, adding and substituting from equations (B1) and (B2),

$$Z_0 Q_B = Z_0 Q_{+B} + Z_0 Q_{-B} = P_{+A}e^{-i\beta} - P_{-A}e^{+i\beta}$$

Substituting from equation (B6) and (B7) and simplifying give

$$Z_0 Q_B = Z_0 Q_A \cosh i\beta - P_A \sinh i\beta \tag{B11}$$

Solving equation (B10) and (B11) for P_A and Z_0Q_A gives

$$P_A = P_B \cosh i\beta + Z_0Q_B \sinh i\beta \tag{B12}$$

$$Z_0Q_A = Z_0Q_B \cosh i\beta + P_B \sinh i\beta \tag{B13}$$

Equations applicable to the section from C to D are obtained by changing subscripts.

Details of Derivation of Equations (19) to (22)

From equations (6) and (17),

$$V\rho c = \frac{1}{z_m} [P_E(1 - \epsilon) - P_C] \tag{B14}$$

Substituting the expression for P_C from equation (9) gives

$$V\rho c = \frac{1}{z_m} [P_E(1 - \epsilon) - (P_D \cosh i\beta + Z_0Q_D \sinh i\beta)] \tag{B15}$$

Using equations (14), (15), and (16),

$$V\rho c = \frac{1}{z_m}\left[P_E(1 - \epsilon) - \left(P_E \cosh i\beta + \frac{P_E}{Z_E} Z_0 \sinh i\beta + VSZ_0 \sinh i\beta\right)\right] \tag{B16}$$

Using equations (4), (17), and (18) and rearranging result in

$$V\rho c \left(1 + \frac{\sinh i\beta}{z_m}\right) = \frac{P_E}{z_m} \left(1 - \epsilon - \cosh i\beta - \frac{\sinh i\beta}{z_E}\right) \tag{B17}$$

The transfer function T is given by (eq. (3))

$$T = \frac{V\rho c}{P_E} = \frac{1 - \epsilon - \cosh i\beta - \dfrac{\sinh i\beta}{z_E}}{z_m + \sinh i\beta} \tag{B18}$$

Letting $\Upsilon = \Upsilon_x + i\Upsilon_y$ and $z_m = z_{mx} + iz_{my}$ and separating the real and imaginary parts,

$$\Upsilon_x + i\Upsilon_y = \frac{z_{mx}(1 - \epsilon - \cos\beta) - \frac{\sin\beta}{z_E}(z_{my} + \sin\beta)}{z_{mx}^2 + (z_{my} + \sin\beta)^2}$$

$$+ i\left[\frac{-(z_{my} + \sin\beta)(1 - \epsilon - \cos\beta) - \frac{z_{mx}\sin\beta}{z_E}}{z_{mx}^2 + (z_{my} + \sin\beta)^2}\right] \qquad (19a)$$

From equation (9),

$$P_C = P_D \cosh i\beta + Z_0 Q_D \sinh i\beta \qquad (B19)$$

$$Z_0 Q_C = Z_0 Q_D \cosh i\beta + P_D \sinh i\beta \qquad (B20)$$

Substituting from equations (12) to (16) in (B19) and (B20), respectively, and simplifying using equation (3) and (18) result in

$$P_B = P_E \cosh i\beta + Z_0\left(\frac{P_E}{Z_E} + VS\right)\sinh i\beta = P_E\left[\cosh i\beta + \left(\frac{1}{z_E} + \Upsilon\right)\sinh i\beta\right] \qquad (B21)$$

$$Z_0 Q_B = -Z_0 VS + Z_0\left(\frac{P_E}{Z_E} + VS\right)\cosh i\beta + P_E \sinh i\beta$$

$$= P_E\left[\left(\frac{1}{z_E} + \Upsilon\right)\cosh i\beta + \sinh i\beta - \Upsilon\right] \qquad (B22)$$

From equation (8),

$$P_A = P_B \cosh i\beta + Z_0 Q_B \sinh i\beta$$

Substituting from equations (B21) and (B22),

$$\frac{P_A}{P_E} = \left[\cosh i\beta + \left(\frac{1}{z_E} + \Upsilon\right) \sinh i\beta\right] \cosh i\beta + \left[\left(\frac{1}{z_E} + \Upsilon\right) \cosh i\beta + \sinh i\beta - \Upsilon\right] \sinh i\beta$$

and simplifying,

$$\Phi = \cosh i2\beta + \frac{1}{z_E} \sinh i2\beta + \Upsilon(\sinh i2\beta - \sinh i\beta) \qquad (B23)$$

Separating real and imaginary parts,

$$\Phi_x + i\Phi_y = \cos 2\beta - \Upsilon_y(\sin 2\beta - \sin \beta) + i\left[\frac{\sin 2\beta}{z_E} + \Upsilon_x(\sin 2\beta - \sin \beta)\right] \qquad (20a)$$

From equation (8),

$$Z_0 Q_A = Z_0 Q_B \cosh i\beta + P_B \sinh i\beta$$

Substituting from equations (B21) and (B22) and simplifying as before,

$$\frac{Z_0 Q_A}{P_E} = \left[\left(\frac{1}{z_E} + \Upsilon\right)\cosh i\beta + \sinh i\beta - \Upsilon\right] \cosh i\beta + \left[\cosh i\beta + \left(\frac{1}{z_E} + \Upsilon\right)\sinh i\beta\right] \sinh i\beta$$

$$\Psi = \sinh i2\beta + \frac{1}{z_E} \cosh i2\beta + \Upsilon (\cosh i2\beta - \cosh i\beta) \qquad (B24)$$

$$\Psi_x + i\Psi_y = \frac{1}{z_E} \cos 2\beta + \Upsilon_x (\cos 2\beta - \cos \beta) + i\left[\sin 2\beta + \Upsilon_y(\cos 2\beta - \cos \beta)\right] \qquad (21a)$$

Equation (22) was obtained directly from

$$z_A = \frac{\Phi}{\Psi}$$

REFERENCES

1. Sabersky, Rolf H.: Effect of Wave Propagation in Feed Lines on Low-Frequency Rocket Instability. Jet Prop., vol. 24, no 3, May-June 1954, pp. 172-174.

2. Chang, S. S. L.: Transient Effects of Supply and Connecting Conduits in Hydraulic Control Systems. Franklin Inst. Jour., vol. 262, no. 6, Dec. 1956, pp. 437-452.

3. Regetz, John D., Jr.: An Experimental Determination of the Dynamic Response of a Long Hydraulic Line. NASA TN D-576, 1960.

4. Moore, Howard: Analysis and Control of Hydraulic Surge. Cook Tech. Rev., vol. 2, no. 2, Aug. 1955.

5. Morse, Philip M.: Vibration and Sound. Second ed., McGraw-Hill Book Co., Inc., 1948.

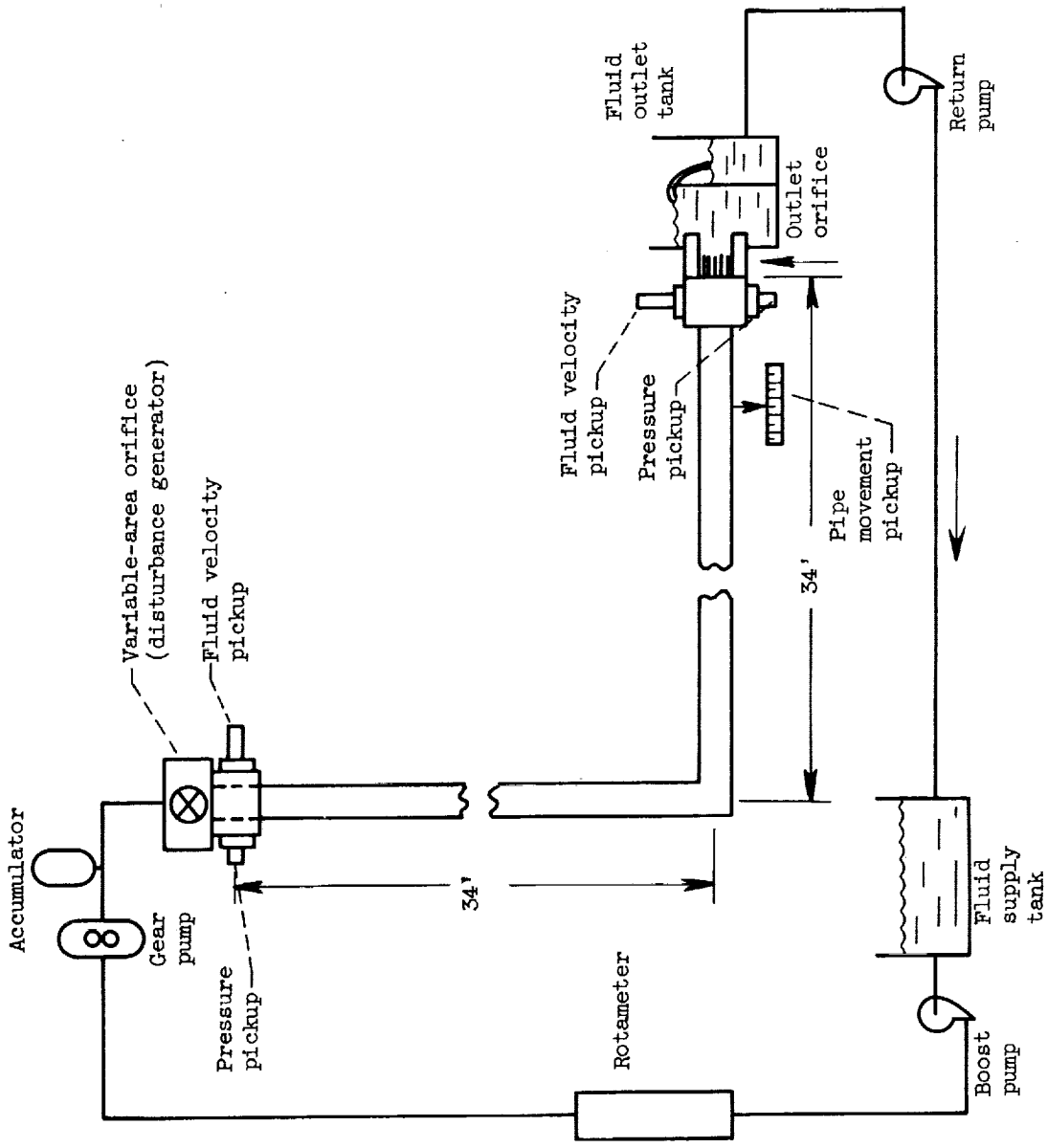

Figure 1. - Hydraulic lines experimental setup.

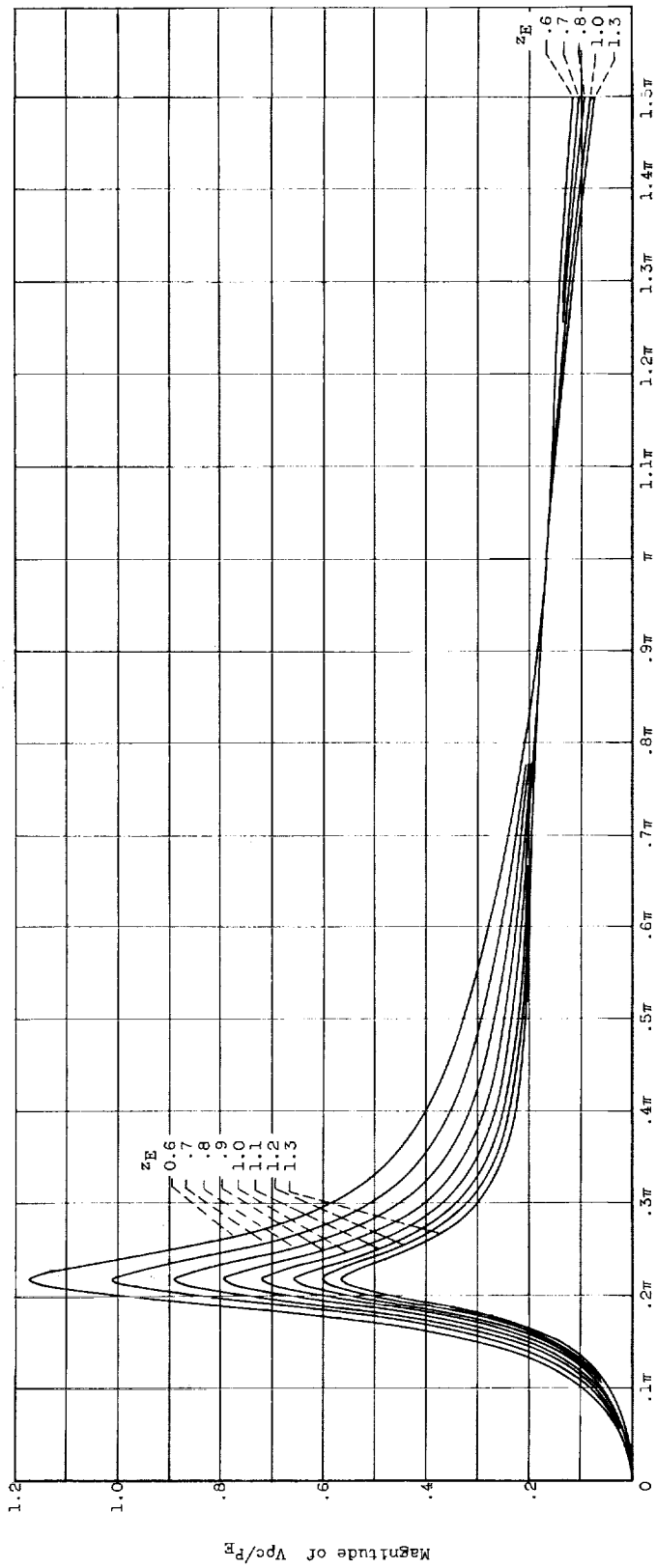

(a) Magnitude of dimensionless downstream pipe-motion admittance.

Figure 3. - Calculated system transfer functions.

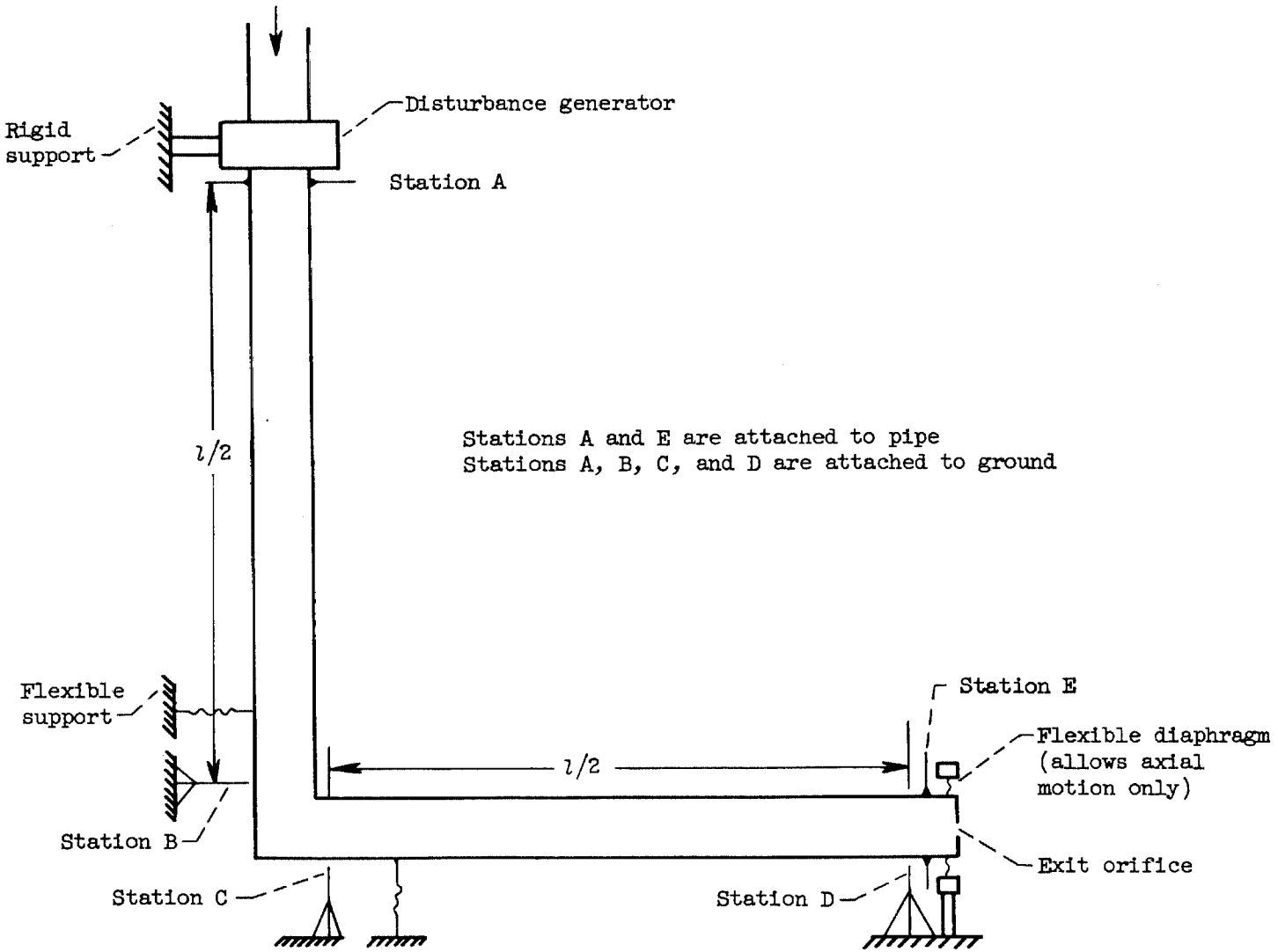

Figure 2. - Experimental system showing reference stations used in analysis.

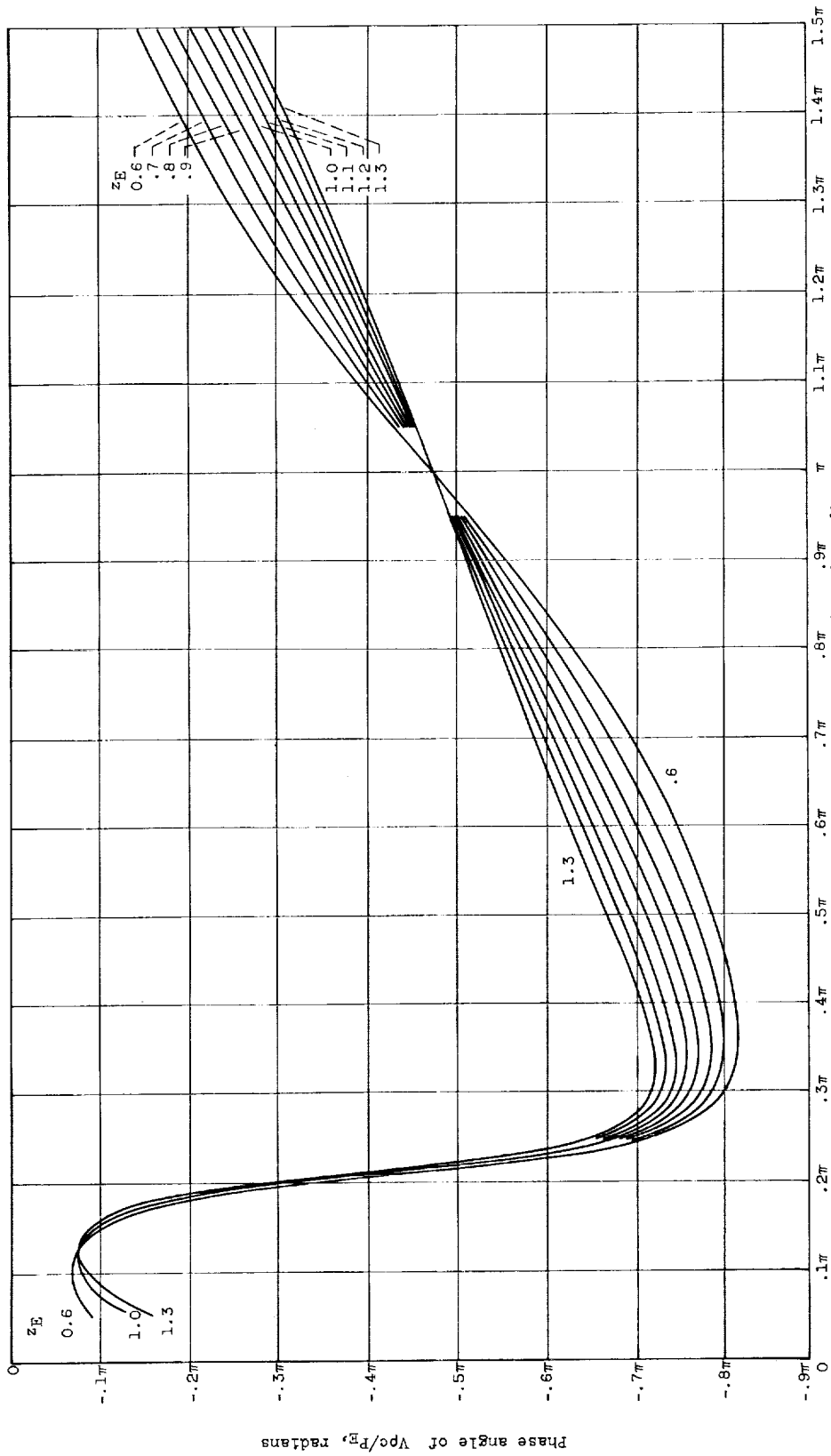

(b) Phase angle of dimensionless downstream pipe-motion admittance.

Figure 3. - Continued. Calculated system transfer functions.

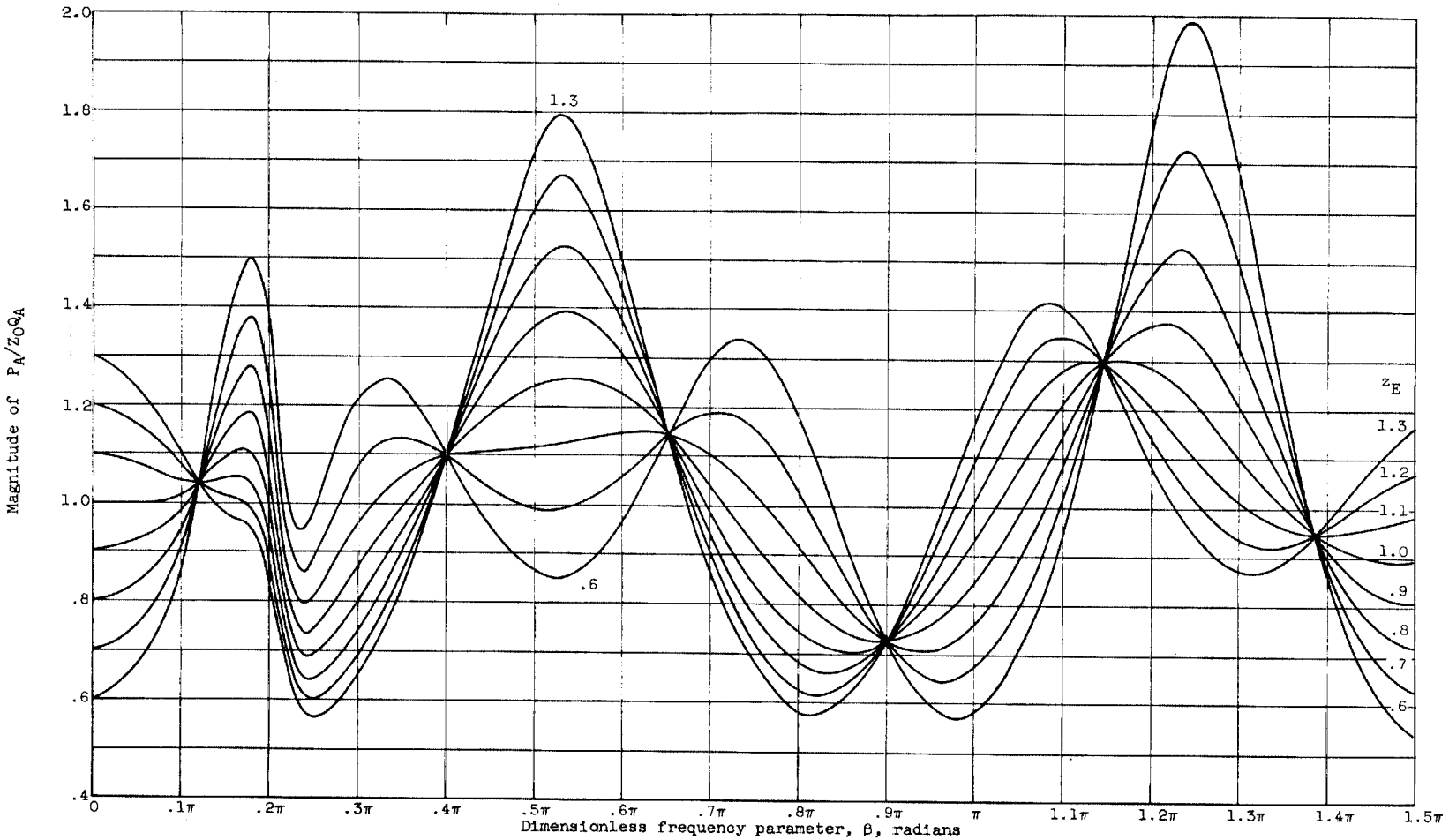

(c) Magnitude of dimensionless upstream impedance.

Figure 3. - Continued. Calculated system transfer functions.

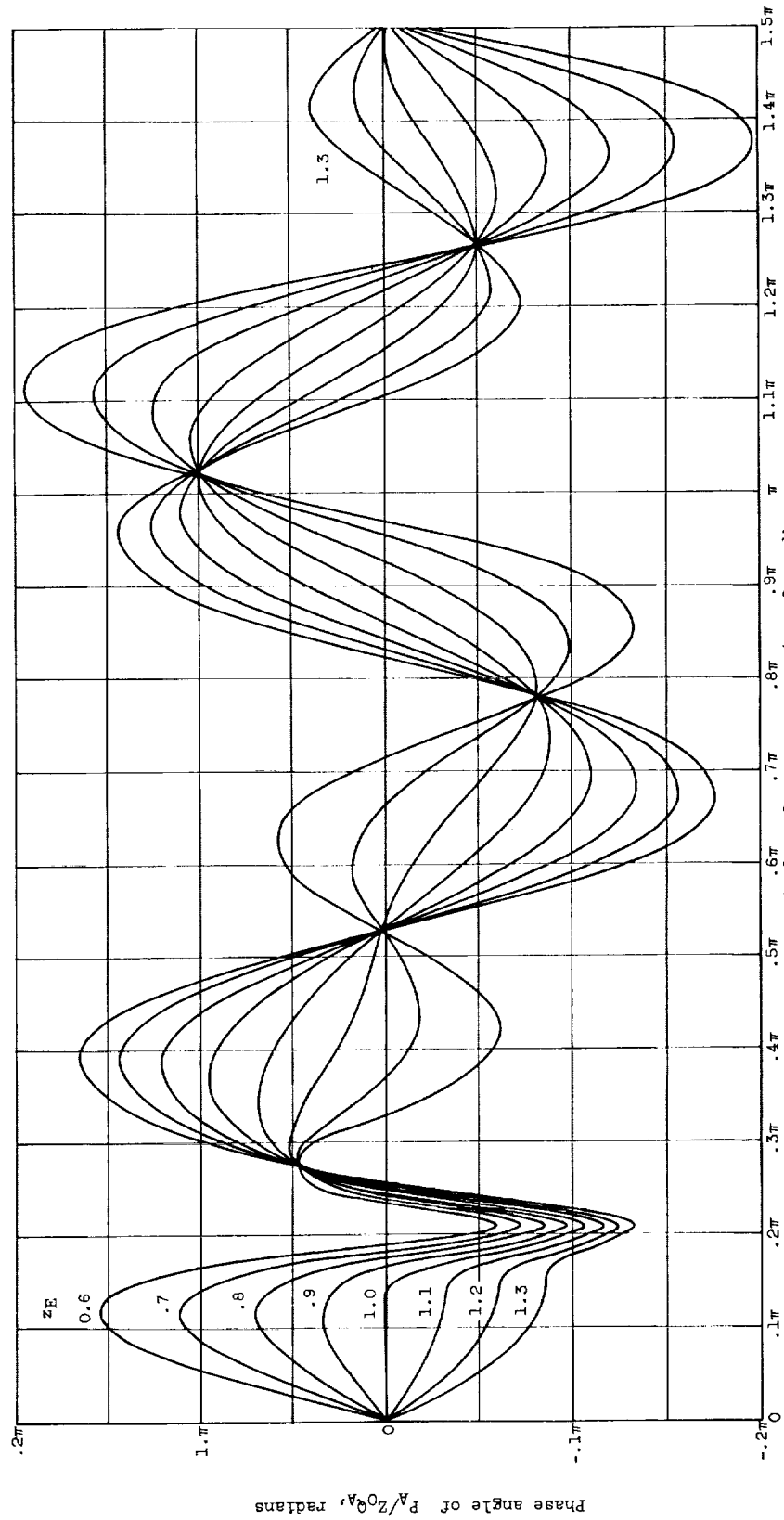

(d) Phase angle of dimensionless upstream impedance.

Figure 3. - Continued. Calculated system transfer functions.

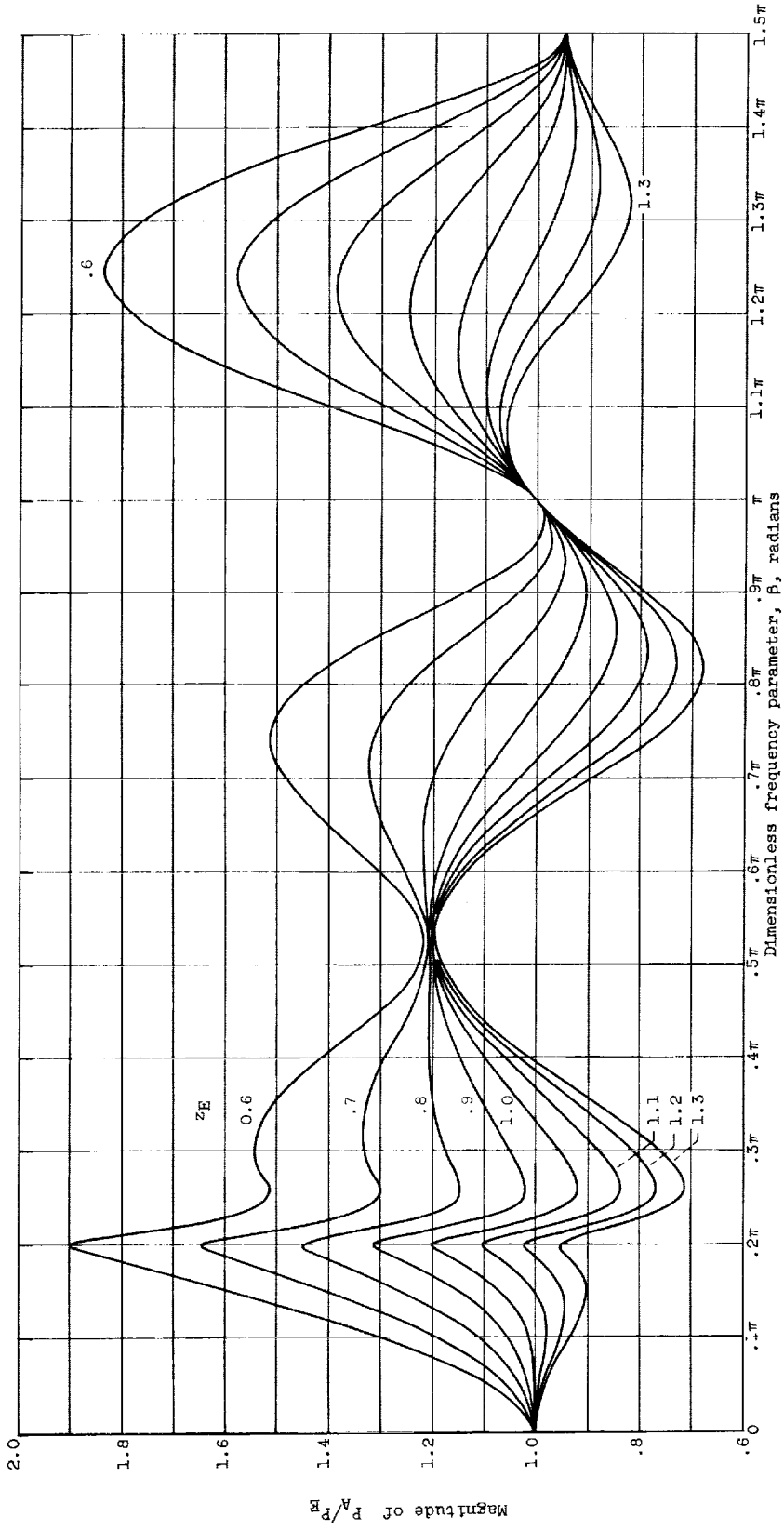

(e) Magnitude of interterminal pressure ratio P_A/P_E.

Figure 3. - Continued. Calculated system transfer functions.

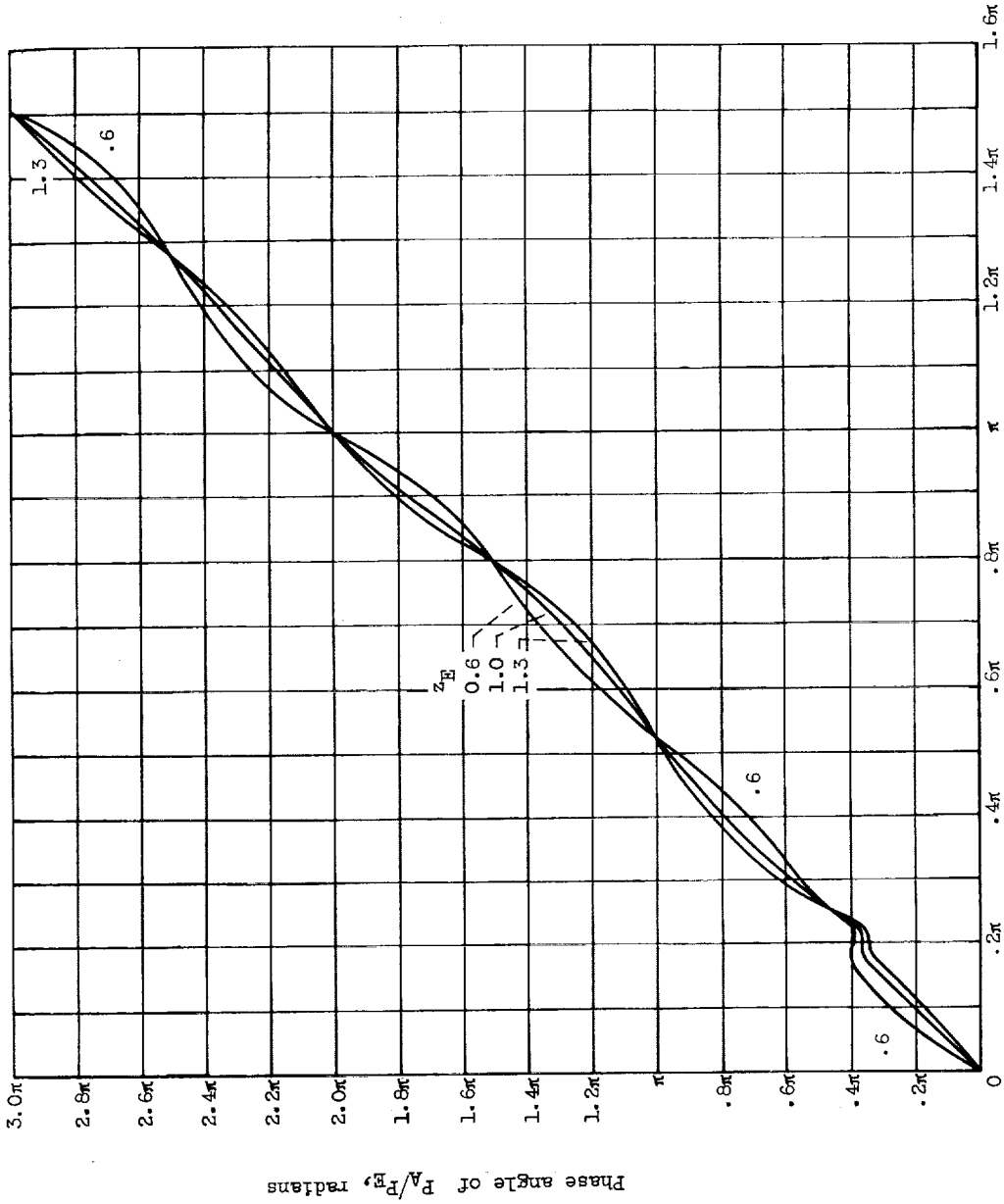

(f) Phase angle of interterminal pressure ratio.

Figure 3. - Concluded. Calculated system transfer functions.

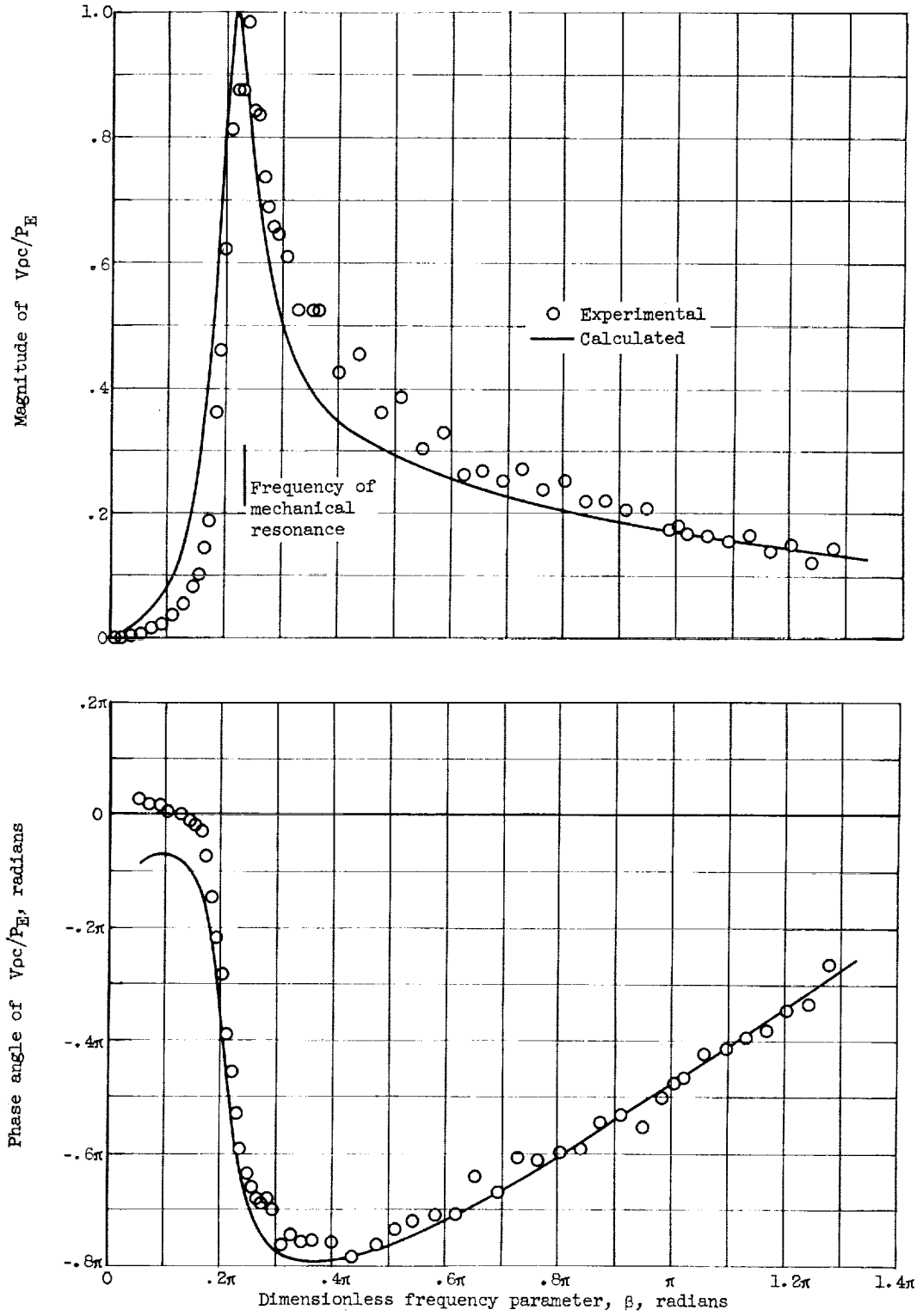

(a) $z_E = 0.715$.

Figure 4. - Dimensionless downstream pipe-motion admittance.

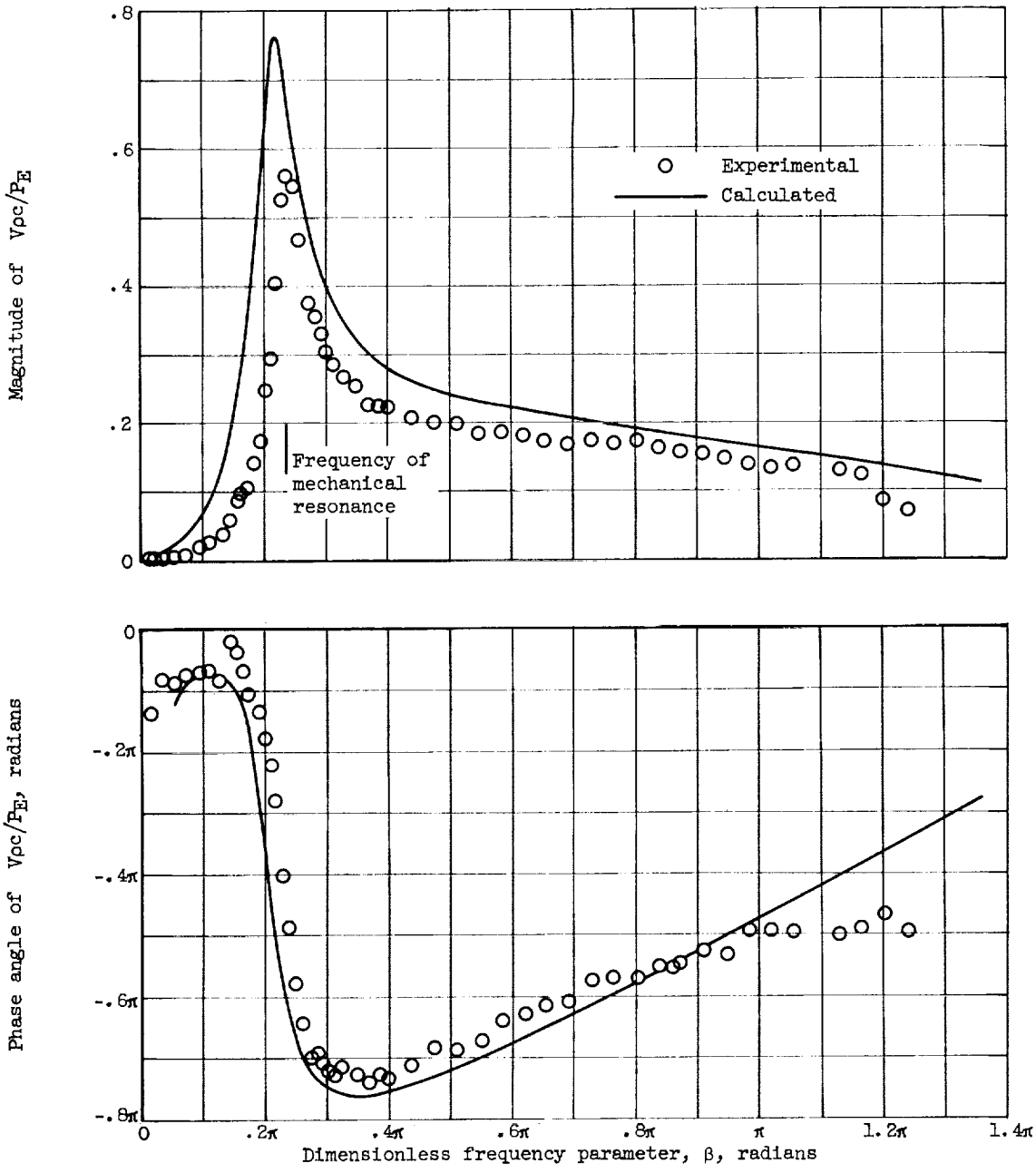

(b) $z_E = 0.94$.

Figure 4. - Continued. Dimensionless downstream pipe-motion admittance.

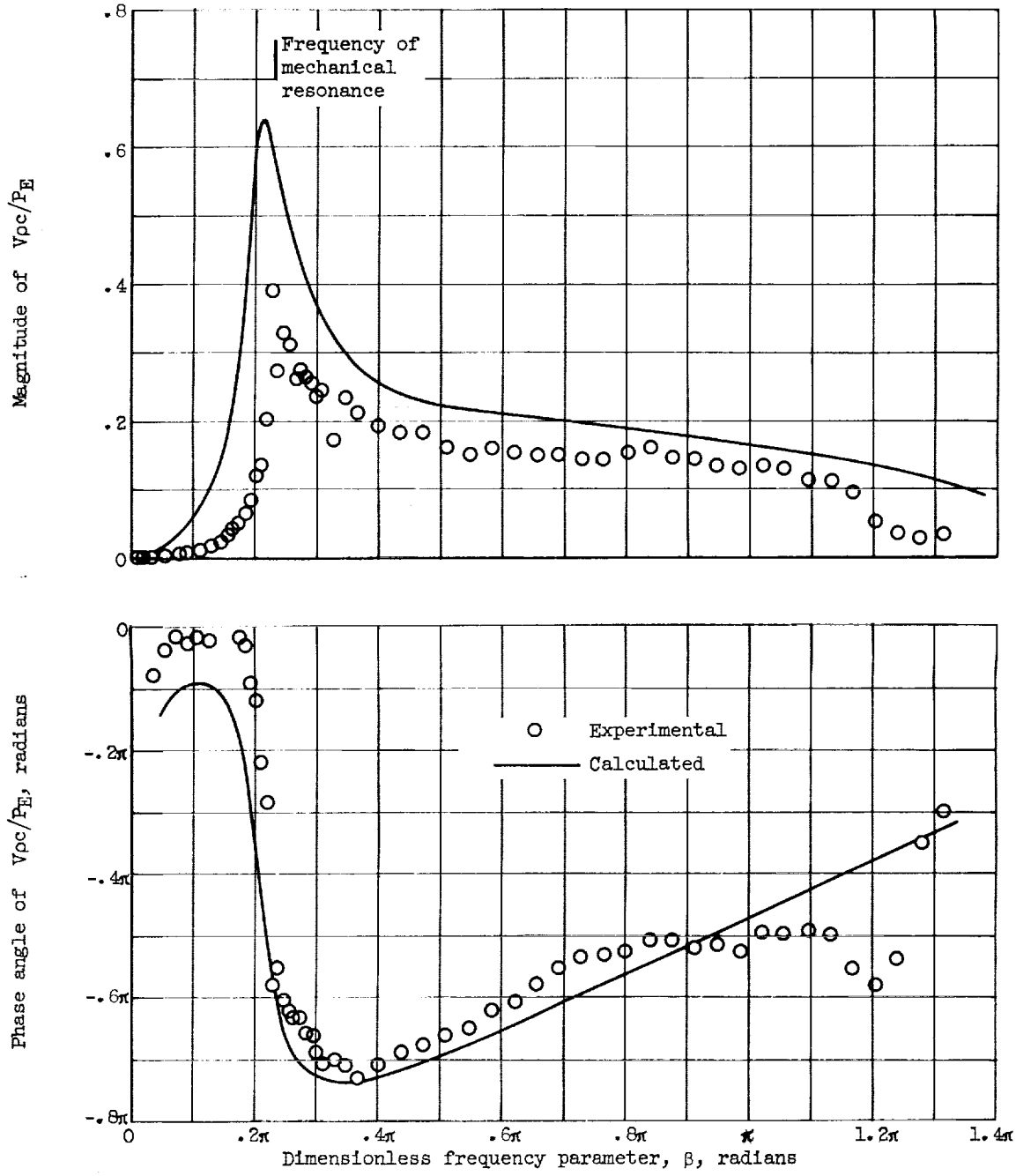

(c) $z_E = 1.13$.

Figure 4. - Concluded. Dimensionless downstream pipe-motion admittance.

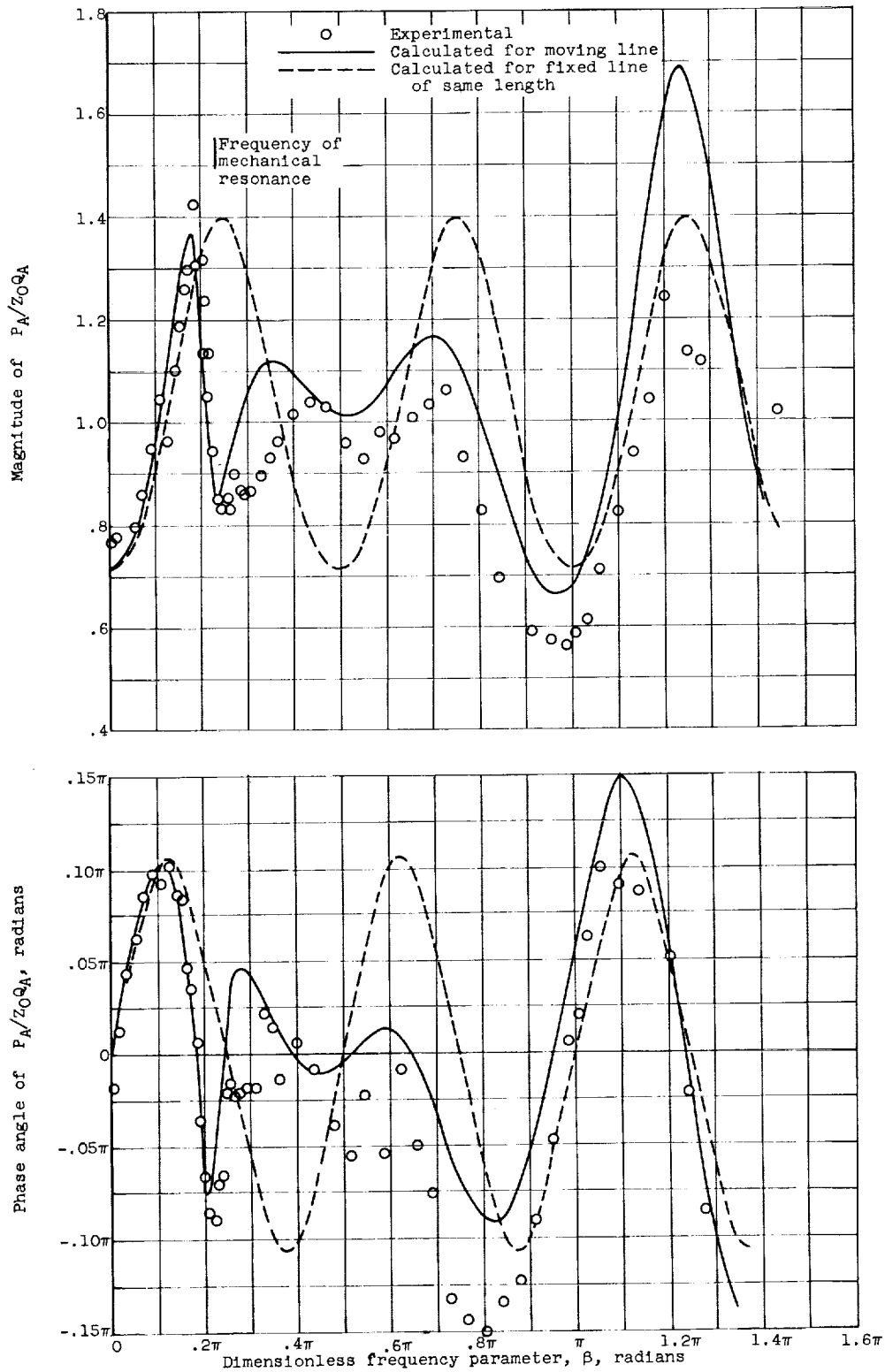

(a) $z_E = 0.715$.

Figure 5. - Dimensionless upstream impedance, z_A, P_A/Z_0Q_A.

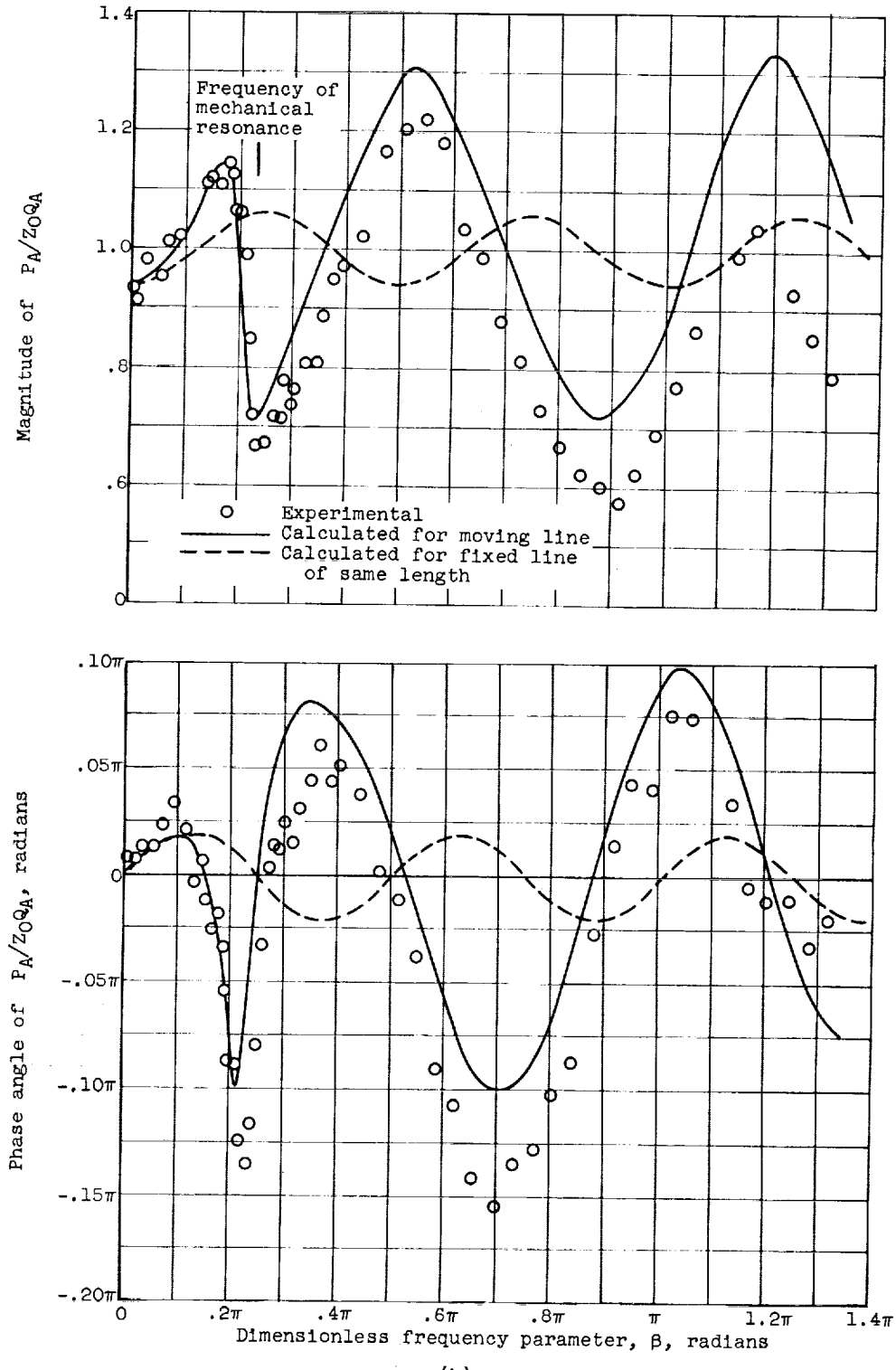

(b) $z_E = 0.94$.

Figure 5. - Continued. Dimensionless upstream impedance, z_A, P_A/Z_0Q_A.

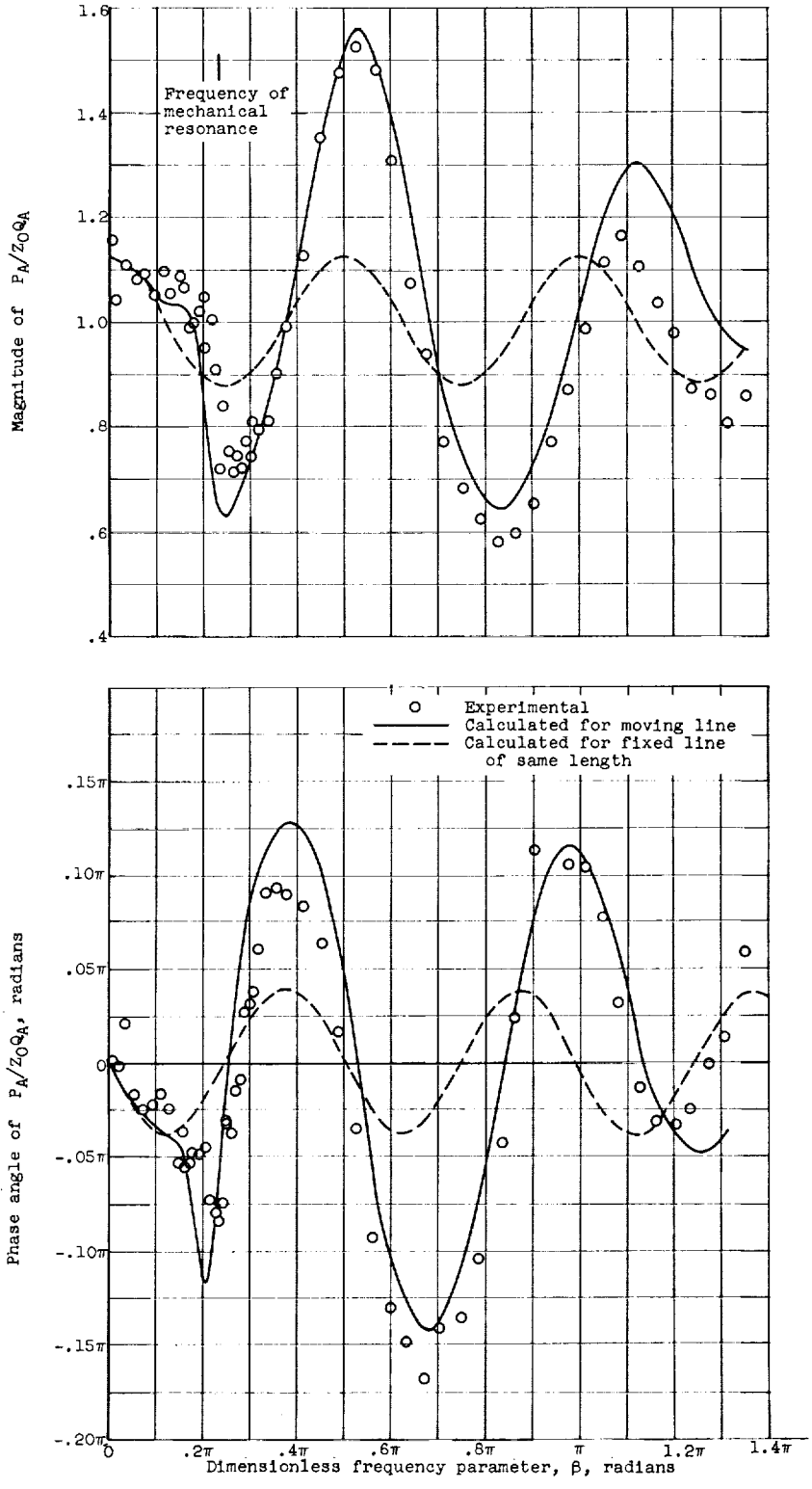

(c) $z_E = 1.13$.

Figure 5. - Concluded. Dimensionless upstream impedance, z_A, P_A/Z_0Q_A.

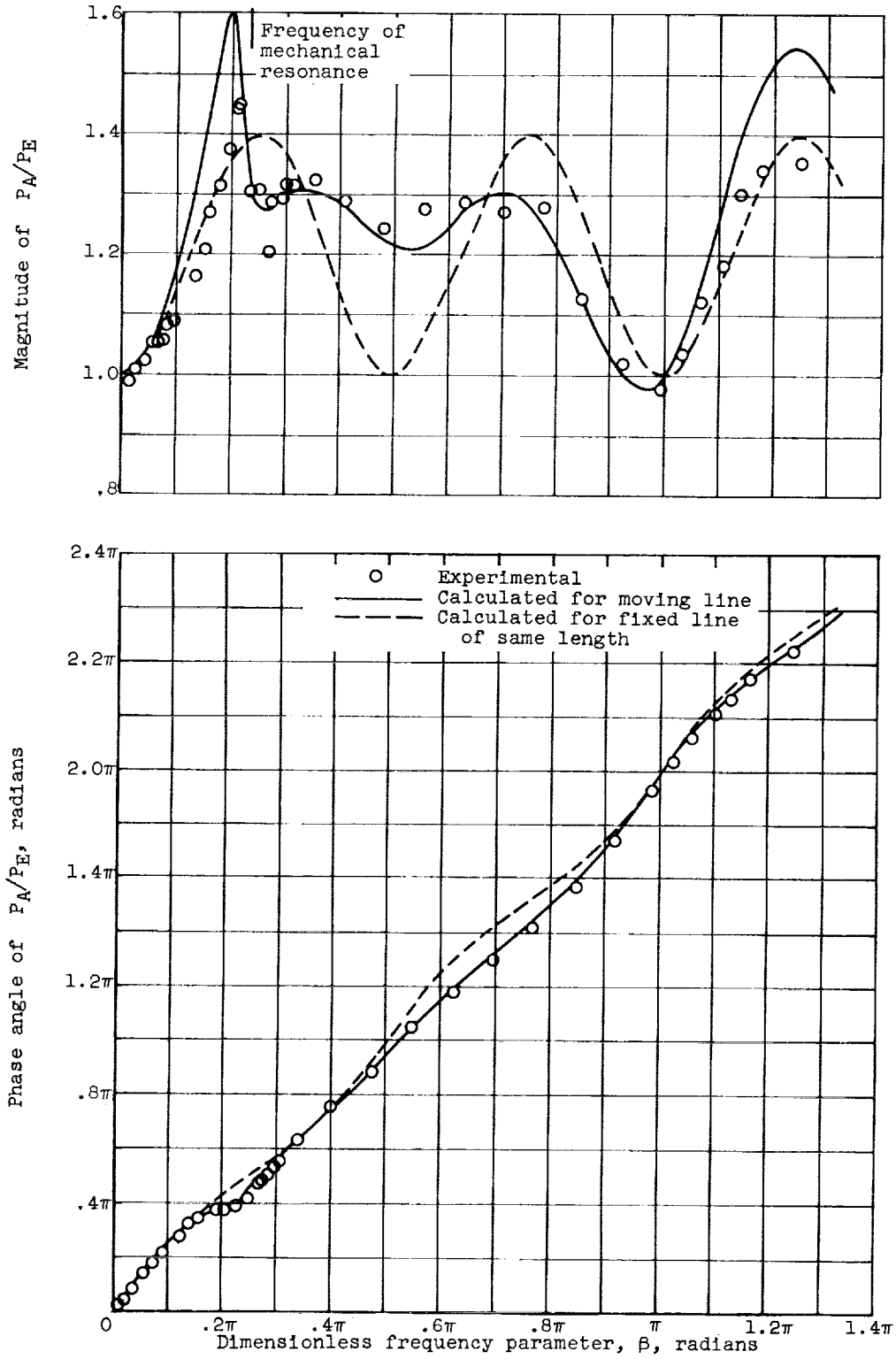

(a) $z_E = 0.715$.

Figure 6. - Interterminal pressure ratio, $\Phi = P_A/P_E$.

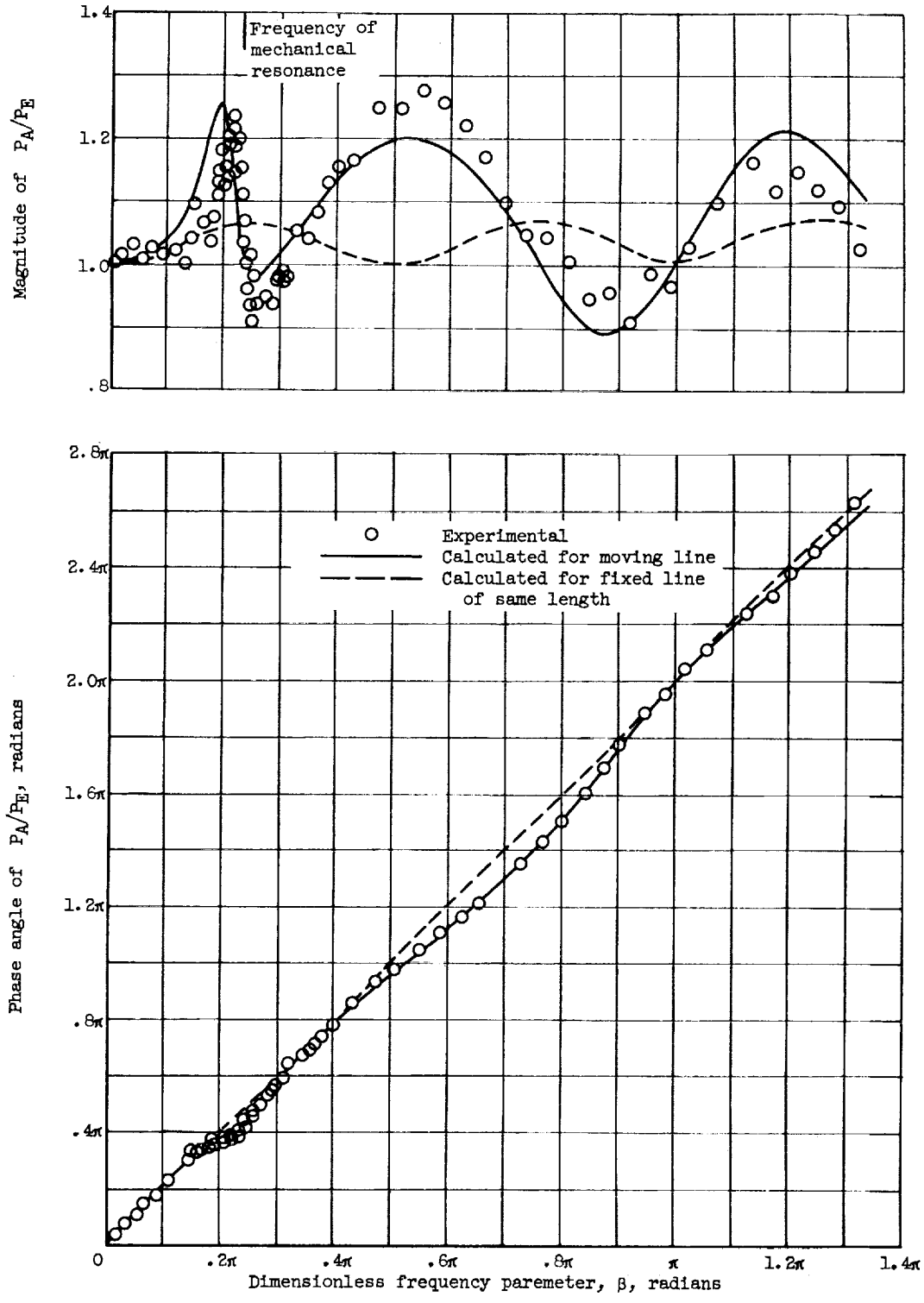

(b) $z_E = 0.94$.

Figure 6. - Continued. Interterminal pressure ratio, $\Phi = P_A/P_E$.

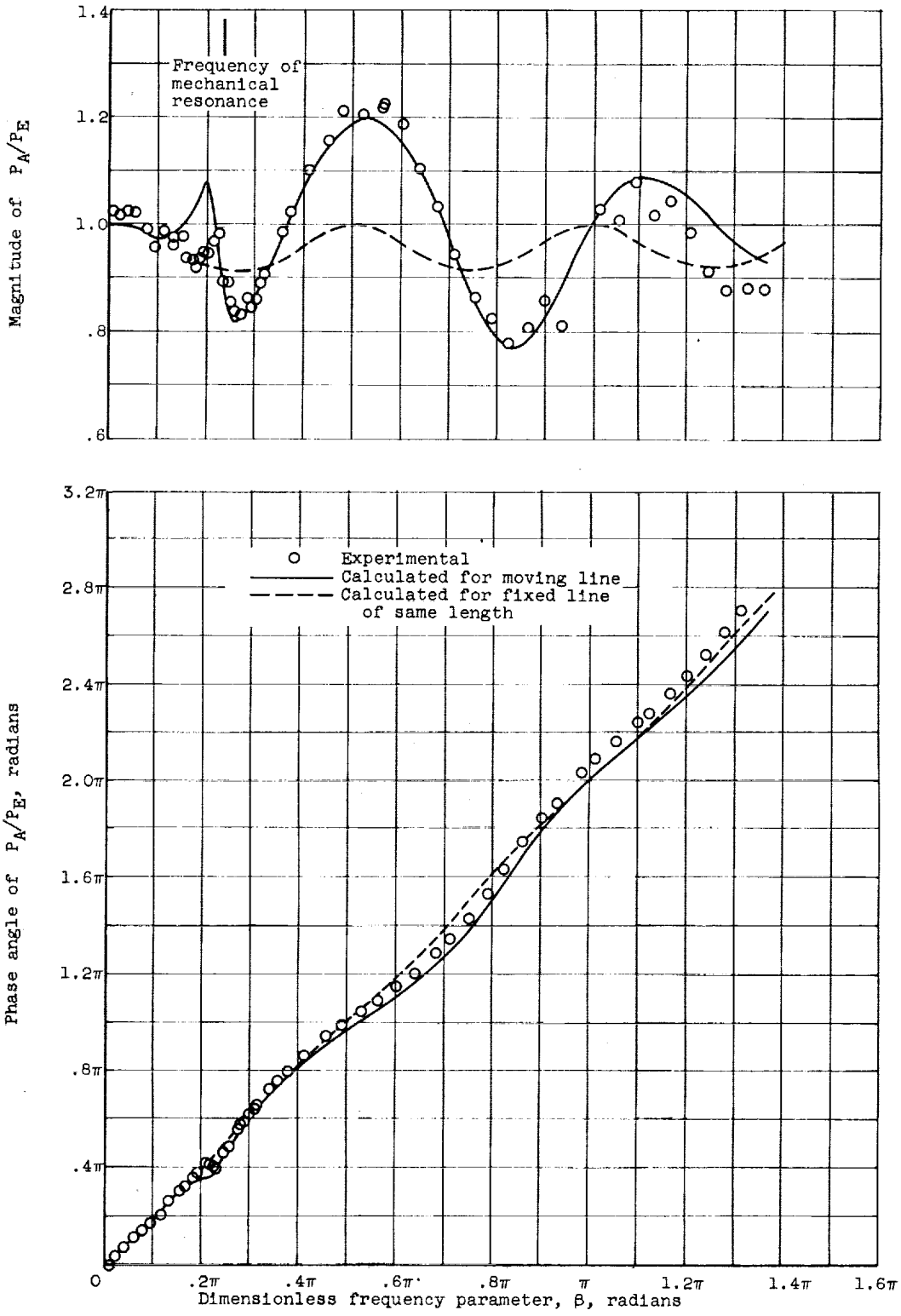

(c) $z_E = 1.13$.

Figure 6. - Concluded. Interterminal pressure ratio, $\Phi = P_A/P_E$.

NASA TN D-1216
National Aeronautics and Space Administration.
STUDY OF A SINUSOIDALLY PERTURBED FLOW IN A LINE INCLUDING A 90° ELBOW WITH FLEXIBLE SUPPORTS. Robert J. Blade, William Lewis, and Jack H. Goodykoontz. July 1962. 38p. OTS price, $1.00. (NASA TECHNICAL NOTE D-1216)

A study is made of the fluid disturbances, within a long line containing a 90° bend, resulting from the coupling between acoustic waves in the flowing fluid and the motion of the line itself due to unbalanced pressure forces on the line. A method of analysis is given, and experimental data are compared with theoretical calculations. Data are presented as transfer functions of several relations as functions of frequency for various conditions. The pipe motion is shown to be a major factor in determining the resultant wave motion. The elbow per se caused no noticeable reflection, attenuation, or phase shift in the fluid waves.

I. Blade, Robert J.
II. Lewis, William
III. Goodykoontz, Jack H.
IV. NASA TN D-1216

(Initial NASA distribution: 20, Fluid mechanics.)

NASA

NASA TN D-1216
National Aeronautics and Space Administration.
STUDY OF A SINUSOIDALLY PERTURBED FLOW IN A LINE INCLUDING A 90° ELBOW WITH FLEXIBLE SUPPORTS. Robert J. Blade, William Lewis, and Jack H. Goodykoontz. July 1962. 38p. OTS price, $1.00. (NASA TECHNICAL NOTE D-1216)

A study is made of the fluid disturbances, within a long line containing a 90° bend, resulting from the coupling between acoustic waves in the flowing fluid and the motion of the line itself due to unbalanced pressure forces on the line. A method of analysis is given, and experimental data are compared with theoretical calculations. Data are presented as transfer functions of several relations as functions of frequency for various conditions. The pipe motion is shown to be a major factor in determining the resultant wave motion. The elbow per se caused no noticeable reflection, attenuation, or phase shift in the fluid waves.

I. Blade, Robert J.
II. Lewis, William
III. Goodykoontz, Jack H.
IV. NASA TN D-1216

(Initial NASA distribution: 20, Fluid mechanics.)

NASA

NASA TN D-1216
National Aeronautics and Space Administration.
STUDY OF A SINUSOIDALLY PERTURBED FLOW IN A LINE INCLUDING A 90° ELBOW WITH FLEXIBLE SUPPORTS. Robert J. Blade, William Lewis, and Jack H. Goodykoontz. July 1962. 38p. OTS price, $1.00. (NASA TECHNICAL NOTE D-1216)

A study is made of the fluid disturbances, within a long line containing a 90° bend, resulting from the coupling between acoustic waves in the flowing fluid and the motion of the line itself due to unbalanced pressure forces on the line. A method of analysis is given, and experimental data are compared with theoretical calculations. Data are presented as transfer functions of several relations as functions of frequency for various conditions. The pipe motion is shown to be a major factor in determining the resultant wave motion. The elbow per se caused no noticeable reflection, attenuation, or phase shift in the fluid waves.

I. Blade, Robert J.
II. Lewis, William
III. Goodykoontz, Jack H.
IV. NASA TN D-1216

(Initial NASA distribution: 20, Fluid mechanics.)

NASA

NASA TN D-1216
National Aeronautics and Space Administration.
STUDY OF A SINUSOIDALLY PERTURBED FLOW IN A LINE INCLUDING A 90° ELBOW WITH FLEXIBLE SUPPORTS. Robert J. Blade, William Lewis, and Jack H. Goodykoontz. July 1962. 38p. OTS price, $1.00. (NASA TECHNICAL NOTE D-1216)

A study is made of the fluid disturbances, within a long line containing a 90° bend, resulting from the coupling between acoustic waves in the flowing fluid and the motion of the line itself due to unbalanced pressure forces on the line. A method of analysis is given, and experimental data are compared with theoretical calculations. Data are presented as transfer functions of several relations as functions of frequency for various conditions. The pipe motion is shown to be a major factor in determining the resultant wave motion. The elbow per se caused no noticeable reflection, attenuation, or phase shift in the fluid waves.

I. Blade, Robert J.
II. Lewis, William
III. Goodykoontz, Jack H.
IV. NASA TN D-1216

(Initial NASA distribution: 20, Fluid mechanics.)

NASA